Biosensors and Bioelectronics 65 (2015) 97–102

Contents lists available at ScienceDirect

Biosensors and Bioelectronics

journal homepage: www.elsevier.com/locate/bios

A signal-off sandwich photoelectrochemical immunosensor using TiO_2 coupled with CdS as the photoactive matrix and copper (II) ion as inhibitor

Yixin Liu, Rongxia Li, Picheng Gao, Yong Zhang, Hongmin Ma, Jiaojiao Yang, Bin Du*, Qin Wei*

Key Laboratory of Chemical Sensing & Analysis in Universities of Shandong, School of Chemistry and Chemical Engineering, University of Jinan, Jinan 250022, PR China

ARTICLE INFO

Article history:
Received 11 July 2014
Received in revised form
30 September 2014
Accepted 8 October 2014
Available online 19 October 2014

Keywords:
Sandwich
Photoelectrochemical biosensor
Signal-off strategy
Cu^{2+} inhibitor

ABSTRACT

In this work, a novel sandwich photoelectrochemical (PEC) biosensor was developed based on a signal-off strategy using TiO_2 coupled with CdS quantum dots (QDs) as the photoactive matrix and copper (II) ion (Cu^{2+}) as inhibitor. TiO_2/CdS modified indium tin oxide (ITO) electrode was employed for primary antibody (Ab_1) immobilization and the subsequent sandwich-type antibody–antigen (Ab–Ag) affinity interactions. Flower-like copper oxide (CuO) was used as labels of secondary antibody (Ab_2) and immobilized on the modified electrode via specific affinity interactions between Ab_2 and Ag. Cu^{2+} was released by dissolving CuO with HCl, and then reacted with CdS to form Cu_xS ($x=1$, 2), which would create new energy levels for electron–hole recombination and resulted in a decrease of the photocurrent. CuO, as the labels of Ab_2, was first applied in PEC biosensor based on the signal-off strategy of the Cu^{2+} for CdS. Greatly enhanced sensitivity was achieved through the coupling of CdS QDs with TiO_2. Besides, the introduction of polythiophene (PT-Cl) on the surface of TiO_2 made the PEC signal more stable. Under 405 nm irradiation at 0.1 V, the PEC biosensor for H–IgG determination exhibited a linear range from 0.1 pg mL^{-1} to 100 ng mL^{-1} with a low detection limit of 0.03 pg mL^{-1}. The proposed biosensor showed high sensitivity, stability and selectivity, which opens up a new promising signal-off PEC platform for future bioassay.

1. Introduction

Photoelectrochemical (PEC) analysis is a newly emerged yet dynamically developing technique for probing various biological events (Haddour et al., 2006; Haddour et al., 2004; Liu et al., 2006; Pardo-Yissar et al., 2003; Tokudome et al., 2005). In the PEC detection process, light is used as the excitation source and the generated photocurrent is used as the detection signal (Lu et al., 2008). Some undesired background signals can be reduced greatly due to the efficient separation of excitation sources and detection signals, thus leading to high sensitivity (Tu et al., 2011). Besides, compared with the optical detection methods such as fluorescence, chemiluminescence (CL) and electrochemiluminescence (ECL), which have to use complex and expensive optical imaging devices and sophisticated image recognition software, the use of electronic detection makes the PEC instrument simple and low-cost (Liang and Guo, 2007; Liang et al., 2007; Liang et al., 2006). Given the advantages mentioned above, the PEC analysis shows great potential application in the field of biosensors. Immunoassays have attracted interest with the expectation of obtaining prompt, accurate, and sensitive immunological response for food safety, environmental monitoring, and medical and clinical diagnosis (Liu et al., 2008; Tang et al., 2008). Some PEC analysis on the determination of anticholera toxin antibody (Haddour et al., 2006; Haddour et al., 2004), α-fetoprotein (Wang et al., 2009a), mouse immunoglobulin G (Wang et al., 2009b) and pentachlorophenol (Kang et al., 2010) have been reported in the past decade. In these investigations, the label-free method, which is based on the direct antibody–antigen affinity without markers, has been chosen for the purpose of saving time and cost (Haddour et al., 2006, 2004; Kang et al., 2010; Wang et al., 2009a, 2009b). Despite the good simplicity of the PEC label-free immunosensor, the sensitivity still needs to be improved due to the low capacity of analyte loading and inability for amplification (Zhao et al., 2011). Hence, the development of a sandwich PEC immunosensor with makers might be a useful route for obtaining higher sensitivity.

* Corresponding authors. Fax: +86 531 82765969.
E-mail address: sdjndxwq@163.com (Q. Wei).

http://dx.doi.org/10.1016/j.bios.2014.10.020
0956-5663/

Quantum dots (QDs) have shown great promising application prospect due to high fluorescence quantum yields, stability against photobleaching and size-controlled luminescence properties (Hojeij et al., 2008; Klimov, 2003; Nirmal and Brus, 1999; Su et al., 2005). Especially, CdS QDs have received much attention because of the ideal band gap (2.25 eV), and it has been successfully used for photoelectrochemical enzyme sensors (Murphy and Coffer, 2002; Pardo-Yissar et al., 2003b; Yildiz et al., 2008). However, the photo-to-current conversion efficiency of CdS nanoparticles was low due to the electron–hole recombination. Due to the demand for ultrasensitive detection, it is necessary to find effective ways to further improve the photo-to-current conversion efficiency of CdS. It was reported that coupling TiO_2 with CdS can greatly improve the photocurrent intensity of CdS due to the enhanced charge separation (Nasr et al., 1998; Sant and Kamat, 2002; Vogel et al., 1994). Polythiophene (PT-Cl) has photochemical and thermal stability under photoirradiation (Lan et al., 2011), which can be supposed to make the PEC signal more stable. In this study, PT-Cl was dropped on TiO_2 film to obtain a photoactive sensing matrix, which then coupled with CdS to improve the photocurrent intensity of CdS.

Several methods of photoelectrochemical selective sensing of Cu^{2+} based on the singal-on/off strategy have been reported (Shen et al., 2011; Wang et al., 2010). Inspired by this thought, our previous work has reported a novel PEC bioassay based on the signal-on effect of Cu^{2+} on the C_3N_4 (Li et al., 2014). Herein, another novel ultrasensitive sandwich PEC biosensor was explored for sensitive and specific detection of H-IgG based on signal-off strategy of Cu^{2+} to CdS QDs. In this work, TiO_2/PT-Cl was first assembled on the ITO electrode and then coupled with CdS through a facile physical process to improve the photocurrent intensity of CdS. After that, the antibody was anchored onto the CdS QDs modified ITO electrode for the subsequent sandwich-type Ab–Ag affinity interactions. Flower-like CuO was employed as label of Ab_2 to release Cu^{2+} while treated with HCl (Qu et al., 2011). Then, Cu_xS would form after the interaction between CdS QDs and Cu^{2+}, which would disrupt the electron transfer from the conduction band of CdS to the surface of ITO electrode and further resulted in a decrease of photocurrent. The photocurrent decreased with the increasing of the concentration of the H-IgG. The established strategy also provided a general consideration for the design of PEC immunosensors in the detection of other biomarkers.

2. Experimental section

2.1. Chemicals and reagents

Cadmium chloride ($CdCl_2 \cdot 2.5H_2O$) was purchased from Sinopharm Chemical Reagent Shanghai Co., Ltd.. Thioglycolic acid (TGA) was obtained from Tianjin Kermel Chemical Reagent Co. ITO glass (resistivity 10 Ω/sq) is obtained from Zhuhai Kaivo Electronic Components Co. Ltd., China. N-hydroxysuccinimide (NHS) and 1-ethyl-3-(3-dimethylaminopropyl) carbodiimide hydrochloride (EDC) were obtained from Aladdin Reagent Database Inc. (Shanghai, China). Human immunoglobulin antigen (H-IgG) and anti-human immunoglobulin (anti-H-IgG) were purchased from Shanghai Guyan technology Co. Ltd.. Glutaraldehyde and Bovine serum albumin (BSA) were obtained from Sigma-Aldrich (Beijing, China). All other chemicals were of analytical reagent grade and used without further purification. Phosphate buffer solution (PBS, pH 7.4, 0.1 mol L^{-1}) was used for the preparation of the antibody and antigen solution and blocking buffer solution. All aqueous solutions were prepared using ultrapure water (Milli-Q, Millipore).

2.2. Apparatus.

Scanning electron microscope (SEM) images were obtained using a field emission SEM (Zeiss, Germany). Fourier transform infrared (FTIR) spectrum was obtained with a Perkin-Elmer 580B spectrophotometer (Perkin-Elmer, United States). Electrochemical impedance spectroscopy (EIS) was performed on an Autolab potentiostat/galvanostat (Zahner, Germany) with a three electrode system in 5.0 mM $[Fe(CN)_6]^{3-/4-}$ solution containing 0.10 M KCl, and recorded with an amplitude of 5 mV over a frequency range of 0.1 Hz to 100 kHz. Photoelectrochemical (PEC) measurements were performed on an electrochemical workstation (Zahner Zennium PP211, Germany). Photocurrent was measured by the current–time curve experimental technique on an photoelectrochemical workstation (Zahner Zennium PP211, Germany) at a bias voltage of 0.1 V with light intensity of 150 W cm^{-2}. The distance between the light source and the electrode was fixed at 10 cm. All experiments were carried out at room temperature using a conventional three electrodes system with an ITO working electrode, a platinum wire counter electrode, and a potassium chloride (KCl) saturated calomel reference electrode (SCE).

2.3. Synthesis of CdS QDs and flower-like CuO nanostructures

In this work, the utilized CdS QDs was synthesized according to the previous report with a slight modification (Wang et al., 2009b). Firstly, 250 μL of TGA was added to 50 mL of 1.0×10^{-2} mol L^{-1} $CdCl_2$ aqueous solution and N_2 was bubbled throughout the solution for 30 min to remove the dissolved O_2. During this period, 1.0 mol L^{-1} NaOH was added to adjust the above solution to the desired pH value of 11. Then, 5.0 mL of 0.1 mol L^{-1} Na_2S aqueous solution was injected into this solution to obtain TGA-capped water-soluble CdS QDs. After that, the mixture was refluxed under N_2 atmosphere for 4 h. Finally, the obtained TGA-capped CdS QDs was stored in a refrigerator at 4 °C for future use.

The utilized CuO was synthesized according to the previous report (Cheng et al., 2011). In the typical synthetic process, 0.125 g of $CuSO_4 \cdot 5H_2O$ and 1 mL of H_2O_2 were dissolved in 20 mL distilled water to form a homogeneous solution. Then, 20 mL of 0.15 mol L^{-1} NaOH aqueous solution was rapidly poured into the above solution at room temperature under vigorous stirring and kept for 15 min. The solution was then transferred into a 50 mL Teflon-sealed autoclave, maintained at 120 °C for 6 h and cooled down to room temperature. The final product was separated by centrifugation, washed with distilled water and absolute ethanol for four times, and dried under vacuum at 50 °C for 12 h. Next, the flower-like CuO was functionalized with amine groups. Briefly, an amount of 0.01 g of the CuO powder was dispersed in 10 mL ethanol/water mixture (19/1, V/V). The pH value of the solution was adjusted to 5 by acetic acid. After addition of 600 μL of APTES, the suspension was sonicated for 20 min, and transferred in an oven at 75 °C for 1 h. The suspension was finally centrifugated and washed with ethanol thrice to remove the unreacted silane.

2.4. Preparation of ITO/TiO_2/PT-Cl/CdS electrode

Before preparation, ITO substrates were cut into 2.5×1.0 cm^2 pieces and then sonicated in acetone, ethanol and distilled water for about 30 min, consecutively. After that, the ITO slices dried under the nitrogen stream for future use.

3 mg of TiO_2 powder was ultrasonically dispersed in 1 mL of distilled water, and then 4 μL of the homogeneous suspension was dropped onto a piece of ITO slice. After drying in air, 4 μL of 2 mg mL^{-1} PT-Cl solution was dropped onto the ITO/TiO_2 electrode and dried at room temperature. Then, the electrode was sintered at 450 °C for 30 min in a muffle furnace to obtain desired

film stability and photocurrent intensity and finally cooled down to room temperature. After that, 4 μL of obtained CdS QDs solution was dropped on TiO_2/PT-Cl film and dried at room temperature. After washed with washing buffer, the ITO/TiO_2/PT-Cl/CdS electrode was obtained successfully.

2.5. Fabrication of the sandwich PEC immunosensor

Anti-H-IgG (Ab_1, 1 μg mL^{-1}) was immobilized onto the ITO/TiO_2/PT-Cl/CdS electrode via the classic EDC coupling reactions between –COOH groups on the surface of the TGA-capped CdS QDs and the $-NH_2$ groups of the Ab_1. In detail, 4 μL EDC/NHS solution containing 1×10^{-2} mol L^{-1} of EDC and 2×10^{-3} mol L^{-1} of NHS in distilled water was dropped on ITO/TiO_2/PT-Cl/CdS electrode for 1 h at room temperature, followed by thoroughly rinsing with washing buffer to wash off the excess EDC and NHS. Subsequently, 4 μL of Ab_1 was spread onto ITO/TiO_2/PT-Cl/CdS electrode at 4 °C in a moisture atmosphere to avoid evaporation of solvent. The electrode was then rinsed with the washing buffer to remove physically adsorbed Ab_1 after incubation for 1 h. After that, 4 μL BSA was incubated on the modified electrode for 1 h at 4 °C to block non-specific binding sites and then washed with the washing buffer thoroughly. Next, 4 μL of H-IgG solution with different concentrations was dropped onto the electrodes and incubated for 1 h at 4 °C followed by washing with washing buffer. After the binding reaction between Ab_1 and Ag, the electrodes were allowed for modification with 4 μL of CuO–Ab_2 bioconjugates for 1 h at 4 °C and then washed thoroughly with washing buffer solution. The resulting electrodes were finally employed as a sandwich PEC immunosensor. For H-IgG analysis, the fabricated immunosensor was treated with 2 μL of HCl (0.5 mol L^{-1}) for 5 min and then applied in PEC measurement.

2.6. Photoelectrochemical detection

Photoelectrochemical detection was carried out in PBS (pH 7.0, 0.1 mol L^{-1}) containing 0.25 mol L^{-1}AA, which served as a sacrificial electron donor during the photocurrent measurement. Photocurrent was measured by the current–time curve experimental technique on a photoelectrochemical workstation at a bias voltage of 0.1 V with light intensity of 150 W cm^{-2}.

3. Results and discussion

As shown in Fig. 1A, the SEM of the CuO illustrated a flower-like morphology, which could provide large surface for loading more antibodies. In addition, as shown in Fig. S2, the thickness of petals was about 50 nm, which means that the flower-like CuO was composed of many thin nanosheets. Fig. 1B shows the FT-IR spectrum of amination-CuO in the wavenumber range of 450–4000 cm^{-1}. The amino group showed a pair of N–H stretching bands in the region of 3300–3500 cm^{-1}, indicating successful functionalization of amination-CuO (Yang et al., 2002). Fig. 1C depicts the UV–vis adsorption of the TGA-capped CdS QDs. The absorption spectrum implies that the CdS QDs have a broad absorption range and is suitable for employed as photoactive substrate. TEM image of TiO_2 NPs (Fig. S3) reveals that the average size of TiO_2 NPs is ~10 nm, which induced large specific surface area, allows sufficient loading of CdS QDs. CdS QDs loaded on the surface of the electrode sufficiently could be contributed to the improvement of the sensitivity.Scheme 1

The photoelectrochemical sensor was developed based on the decreased photocurrent caused by the interaction between Cu^{2+} and CdS QDs. It has been reported that the rapid reduction of Cu^{2+} to Cu^{+} would occur under illumination when Cu^{2+} appeared on the surface of CdS (Isarov and Chrysochoos, 1997). It is known that solubility of Cu_xS ($x=1$, 2) is lower than that of CdS. As a result, Cd^{2+} on the surface of CdS would be replaced by Cu^{2+}/Cu^{+} and resulting in the formation of Cu_xS. The formed Cu_xS on the CdS surface created new energy levels in the band gap below the conduction band of CdS and provided a new channel for electron–hole recombination, which decreased the photocurrent intensity of CdS QDs obviously (Wang et al., 2010). Herein, TiO_2 was coupled with CdS to improve the photocurrent intensity of CdS. Once the immunosensor was treated by HCl, Cu^{2+} could be released from CuO-Ab_2 and then inhibit electron transfer of CdS after the interaction between Cu^{2+} and CdS QDs. Therefore, the photocurrent intensity of the immunosensor would decrease with the increase of H-IgG concentration. The possible mechanism for the photoelectrochemical detection is depicted in Scheme 2.

As an effective tool for characterizing the interface properties of electrodes (An et al., 2010), electrochemical impedance spectroscopy (EIS) was used to monitor the fabrication process of the immunosensor. Fig. 2A exhibits the impedance spectra of the electrodes which fabricated in different construction steps. The impedance spectrum includes a semicircle portion at higher frequencies and a linear portion at lower frequencies. The electron-transfer resistance (R_{et}), which equals the semicircle portion, reflects the restricted diffusion of the redox probe through the multilayer system and relates directly to film permeability (Li et al., 2012). The linear portion at lower frequencies corresponds to diffusion-limited process. For the bare ITO electrode, the impedance spectrum exhibited a very small semicircle, indicating a very small R_{et} (curve a). After the modification of TiO_2/PT-Cl and CdS QDs step by step, R_{et} getting much bigger and indicated that the modified layers hindered the access of the redox probe to the electrode surface. Because of the insulating effect of organic molecules, R_{et} gradually increased after the stepwise immobilization of Ab_1 (curve d), BSA (curve e) and Ag (curve f) on the surfaces of TiO_2/PT-Cl/CdS modified ITO, indicating the successful immobilization of every step. Similarly, after the electrode incubated with CuO-Ab_2, R_{et} increased largely. The increases of R_{et} value entirely demonstrated the successful fabrication processes of the immunosensor array.

The fabrication process of the immunosensor can also be monitored by PEC experiments and is shown in Fig. 2B. Curve b presented the photocurrent response of TiO_2/PT-Cl modified ITO electrode. While CdS was subsequently coated, the photocurrent intensity increased to 2.5 times higher than that of TiO_2/PT-Cl electrode thanks to the sensitization effect of CdS (Wang et al., 2009a). Later on, the photocurrent intensity decreased gradually after the Ab_1 anchoring, BSA blocking and Ag specific binding (curves d–f). This could be attributed to the fact that the immobilization of those organics suppressed the electron transfer of the system and partly obstructed AA transfer to the surface of CdS for reaction with the photogenerated holes. When the constructed immunosensor was incubated with CuO-Ab_2, the photocurrent displayed an obvious decrease (curve f), which could be attributed to the modified of CuO-Ab_2 that hindered the interfacial mass and electron transfer largely. Therefore, the photocurrent responses also proved the successful fabrication of the immunosensor.

The photocurrent responses of five modified electrode in the presence and absence of polythiophene were tested respectively. As shown in Table S1, the relative standard deviation (RSD) of ITO/TiO_2/PT-Cl electrode was 1.33%, and the RSD of the ITO/TiO_2 electrode was 9.68%. So, the introduction of polythiophene (PT-Cl) on the surface of TiO_2 made the PEC signal more stable.

In this work, the effects of pH, AA concentration and the applied potential were investigated on the photocurrent response of immunosensor. Fig. S1A shows the influence of pH on the photocurrent responses of the immunosensor, which was operated in

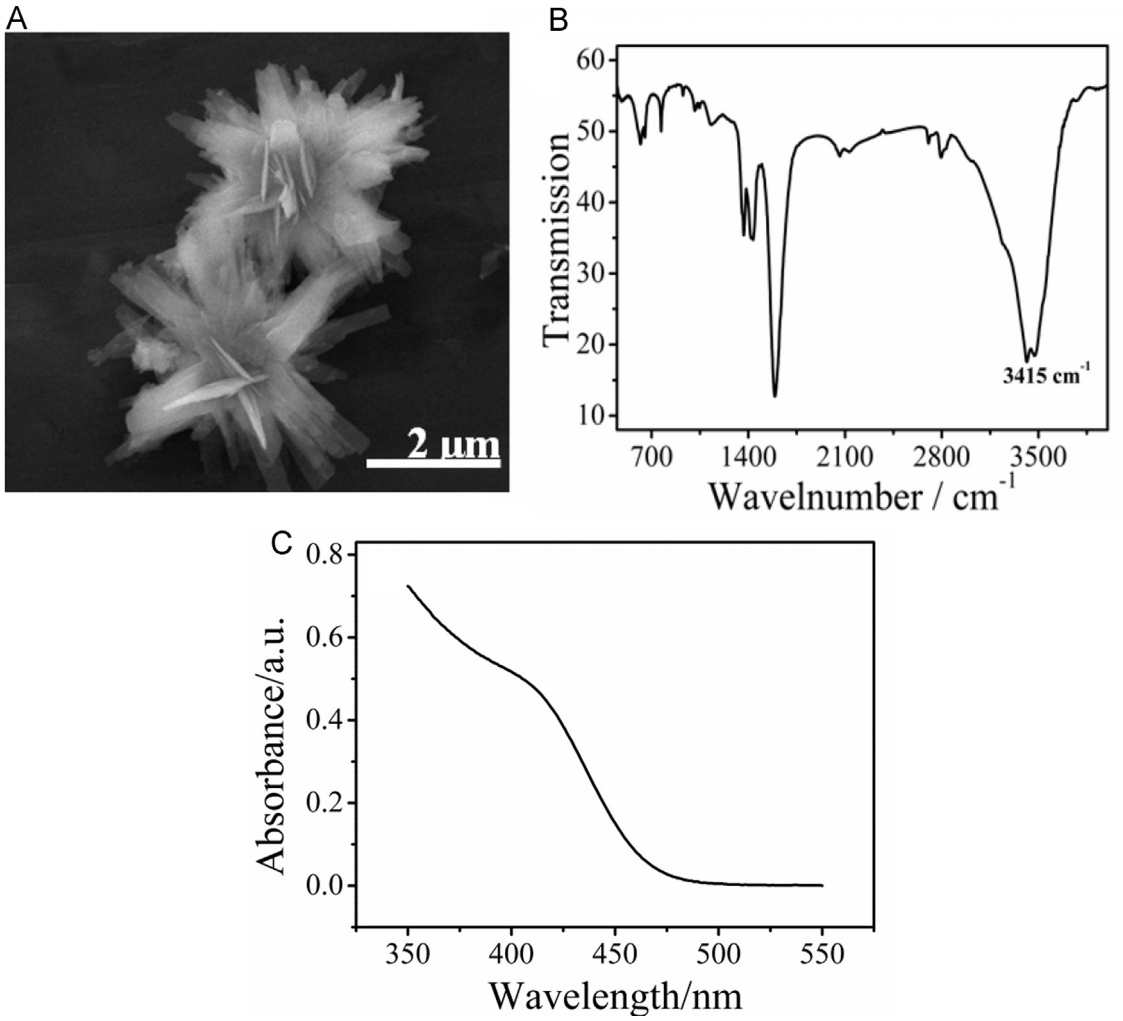

Fig. 1. (A) SEM image of amination-CuO; (B) FT-IR spectra of and amination-CuO; (C) UV–vis adsorption of the CdS QDs aqueous solution.

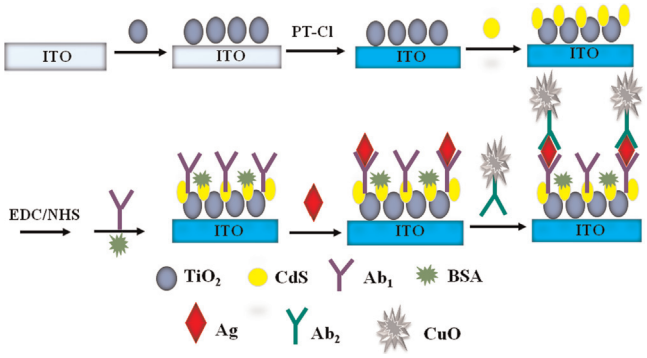

Scheme 1. Fabrication process of the photoelectrochemical immunosensor.

PBS with different pH values ranging from 5.0 to 8.5. The photocurrent responses increased with increasing pH up to 7.0. So the pH 7.0 was selected as the optimum acidity value in subsequent PEC tests. The concentration of ascorbic acid (AA) has significant effect on the sensing performance. As shown in Fig. S1B, with the increase of concentration of AA, the photocurrent intensity increased and reached a plateau at 0.25 mol L^{-1}. Thus, 0.25 moL L^{-1} AA was selected as the optimal concentration. The applied potential was also an important parameter for producing photocurrent. As shown in Fig. S1C, when the irradiation wavelength was 405 nm, the photocurrent intensity increased with the applied potential increasing from −0.2 V to 0.1 V and reached its maximum at 0.1 V. Therefore, 0.1 V was selected as the optimal applied potential for the PEC tests.

The degree of photocurrent variation in this PEC immunoassay is directly related to the concentration of target antigen. Hence, by tracking variation of photocurrent that monitors the amount of analyte, a new immunoassay can be accomplished. Fig. 3 shows the derived calibration curve in the presence of different concentrations of H-IgG. The photocurrent decreases with the increase of the concentration of H-IgG. As shown in Fig. 3, the decrement of the photocurrent was proportional to the logarithm of the concentration of the H-IgG ranging from 0.1 pg mL^{-1} to 100 ng mL^{-1} with a correlation coefficient of 0.981, and the equation of the calibration curve is $\Delta I = 1.5574 + 0.2043 \lg c$. The limit of detection (LOD) was 0.03 pg mL^{-1} ($S/N = 3$). It was comparable and even better than those of many reported immunoassay methods for H-IgG, such as flow-injection electrochemical immunoassay (LOD, 120 μg mL^{-1}) (Tang et al., 2009), electrochemical immunoassay (LOD, 25 ng mL^{-1}) (Zarei et al., 2012), time-resolved fluoroimmunoassay (LOD, 5 ng mL^{-1}) (Niu et al., 2011) and chemiluminescence resonance energy transfer-based immunoassay (LOD, 4.35 ng mL^{-1}) (Qin et al., 2012), which is a promising potential method for determination of H-IgG in clinic.

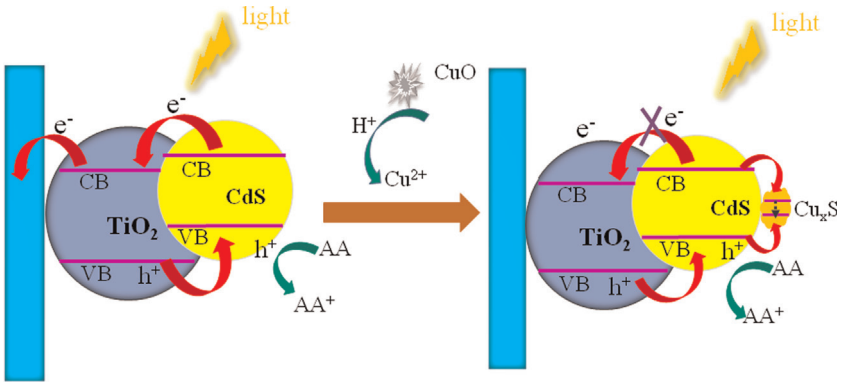

Scheme 2. Schematic illustration of the decreased photocurrent mechanism in the absence and presence of Cu^{2+}.

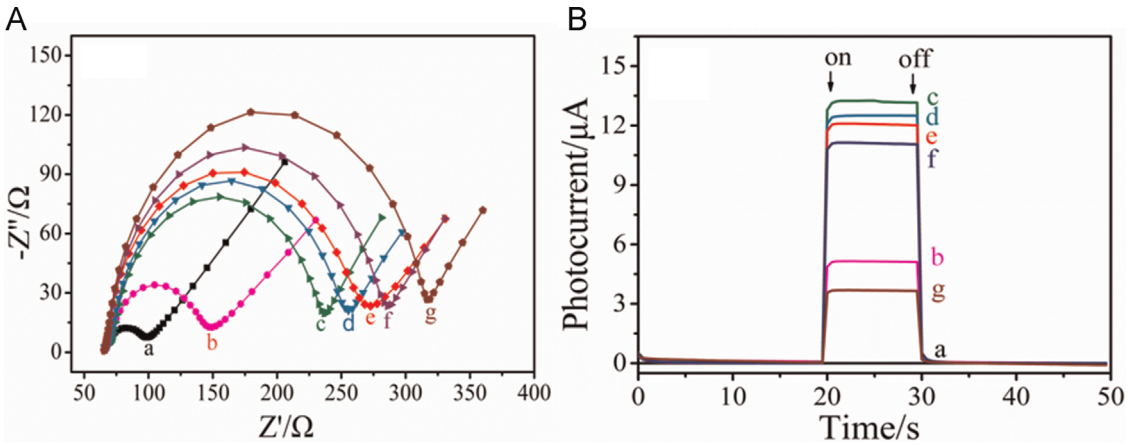

Fig. 2. (A) Nyquist plots of electrochemical impedance spectroscopy (EIS) and (B) corresponding photocurrent responses of the modified ITO electrode: (a) ITO, (b) PT-Cl/TiO_2/ITO, (c) CdS/ PT-Cl/TiO_2/ITO, (d) Ab_1/CdS/PT-Cl/TiO_2/ITO, (e) BSA/Ab_1/ CdS/PT-Cl/TiO_2/ITO, (f) H-IgG/ BSA/Ab_1/CdS/PT-Cl/TiO_2/ITO, (g) CuO-Ab_2 /H-IgG/BSA/Ab_1/CdS/PT-Cl/TiO_2/ITO. The EIS spectra was obtained in 5.0 m mol L^{-1} $[Fe(CN)_6]^{3-/4-}$ solution containing 0.10 mol L^{-1} KCl. The PEC tests were performed in 0.1 mol L^{-1} PBS (pH=7.0) containing 0.25 mol L^{-1} AA with 0.1 V applied potential and 405 nm excitation light.

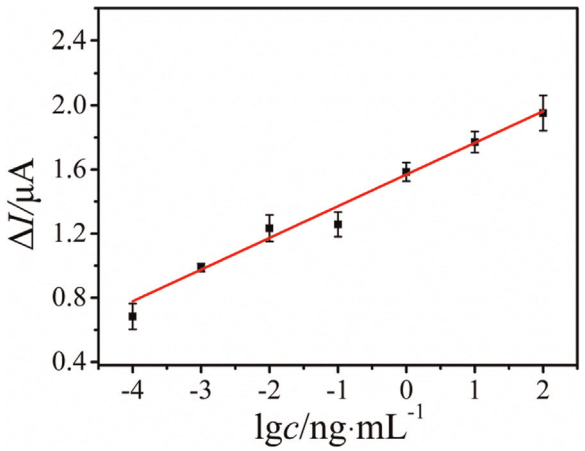

Fig. 3. Effect of different H-IgG concentrations on the differential photocurrent responses, $\Delta I = I_0 - I$, I_0 is the photocurrent of the immunosensor without Ag immobilization and I is the photocurrent of the immunosensor. The photocurrent responses of the immunosensor were measured after treating with HCl. The PEC tests were performed in 0.1 mol L^{-1} PBS (pH=7.0) containing 0.25 mol L^{-1} AA with 0.1 V applied potential and 405 nm excitation light.

The reproducibility of the biosensor was evaluated by both intra-assay and inter-assay relative standard deviation (RSD). Analyzed from the experimental results, the intra-assay RSDs were 3.7%, 3.2% and 2.8% towards 0.1, 1, and 10 ng mL^{-1} of H-IgG, respectively, whereas the inter-assay RSDs of 4.8%, 4.1%, and 3.7% were obtained by measuring the same samples with five electrodes prepared independently at the identical experimental conditions. The results suggested good precision and acceptable reproducibility of this biosensor.

The stability of the designed immunosensor was also evaluated. As shown in Fig.4A, the photocurrent responses were recorded under several on/off irradiation cycles for 500 s and the immunosensor displayed reproducible photocurrent responses without any noticeable variation. The result indicated the structural stability of the developed PEC sensors and photophysical stability in PEC tests and suits for the construction of PEC sensors.

Specificity is an important criterion for immunoassay. To demonstrate that the photocurrent response originated from specific binding, we selected some representative interfering proteins involving alphafetoprotein (AFP), carbohydrate antigen 125 (CA125), bovine serum albumin (BSA) and squamous cell carcinoma antigen (SCCA) for the interference test. The specificity of the immunosensor was evaluated by measuring the photocurrent response of 1 ng mL^{-1} solution of H-IgG containing 100 ng mL^{-1} of interfering substance, respectively. As shown in Fig. 4B, the current variation resulted from the interfering substances was less than 5% of that without interferences, indicating the selectivity of the immunosensor was acceptable. In conclusion, the constructed immunosensor exhibited good stability and selectivity.

To demonstrate the practical application of the immunosensor, the recovery of different concentrations of H-IgG in diluted serum samples was detected using standard addition methods. As shown in Table S2, different concentrations of H-IgG (5.00, 10.0, and

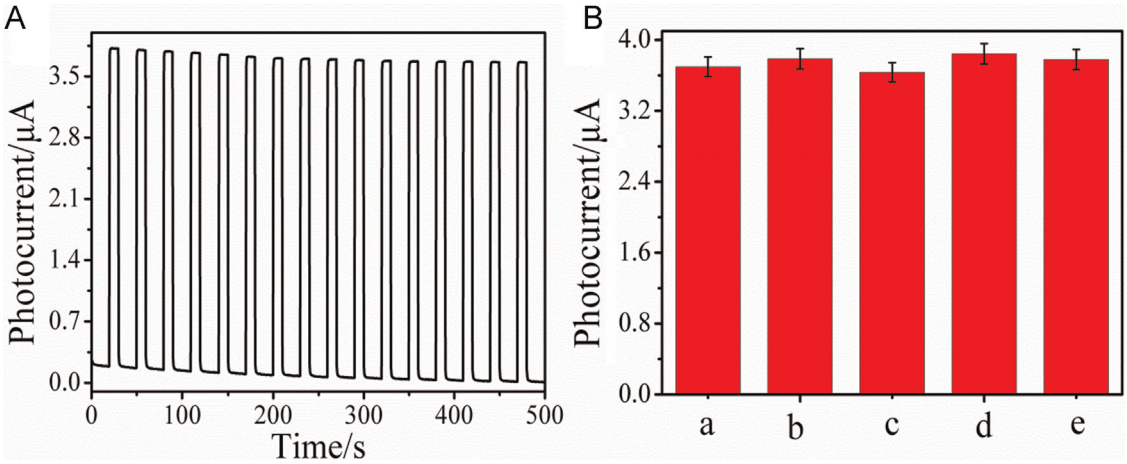

Fig. 4. (A) Time-based photocurrent response of the immunosensor under several on/off irradiation cycles for 500 s. (B) The responses of interference (a) 1.0 ng mL^{-1} H-IgG, (b) 1.0 ng mL^{-1} H-IgG+100 ng mL^{-1} AFP, (c) 1.0 ng mL^{-1} H-IgG+100 ng mL^{-1} CA125, (d) 1.0 ng mL^{-1} H-IgG+100 ng mL^{-1} BSA, (e) 1.0 ng mL^{-1} H-IgG+100 ng mL^{-1} SCCA.

20.0 ng mL^{-1}) were added into diluted serum samples, the average recoveries of the immunosensor were in the range of 97.2–102.0% and the relative standard deviation (RSD) was 3.0–3.5%. Hence, the fabricated immunosensor could be satisfactorily applied to the clinical determination of H-IgG levels in serum samples.

4. Conclusions

In summary, a novel sandwich PEC biosensor was first proposed based on the inhibitory effect of Cu^{2+} to CdS QDs. The formed Cu_xS could disrupt the electron transfer of CdS and result in a decrease of photocurrent. TiO_2 coupled with CdS greatly improved the photocurrent intensity of CdS due to the enhanced charge separation. Cu^{2+} was generated from CuO-labeled Ab while treating with HCl. The well-designed immunoassay exhibited a low detection limit of 0.03 pg mL^{-1} as well as a wider linear range from 0.1 pg mL^{-1} to 100 ng mL^{-1} for H-IgG detection. Besides, the proposed biosensor showed excellent analytical performance for the measurement of H-IgG in diluted serum samples. This proposed PEC immunoassay opens a new perspective for the detection of other cancer biomarkers and has the potential for reliable diagnosis of cancer and other diseases.

Acknowledgments

This study was supported by the National Natural Science Foundation of China (21175057, 21375047 and 21377046), the Science and Technology Plan Project of Jinan (No.201307010) and QW thanks the Special Foundation for Taishan Scholar Professorship of Shandong Province and University of Jinan (No. ts20130937).

Appendix A. Supplementary material

Supplementary data associated with this article can be found in the online version at http://dx.doi.org/10.1016/j.bios.2014.09.014.

References

An, Y.R., Tang, L.L., Jiang, X.L., Chen, H., Yang, M.C., Jin, L.T., Zhang, S.P., Wang, C.G., Zhang, W., 2010. Chem.-Eur. J 16, 14439–14446.
Cheng, Z.P., Xu, J.M., Zhong, H., Chu, X.Z., Song, J., 2011. Mater. Lett. 65, 2047–2050.
Haddour, N., Chauvin, J., Gondran, C., Cosnier, S., 2006. J. Am. Chem. Soc. 128, 9693–9698.
Haddour, N., Cosnier, S., Gondran, C., 2004. Chem. Commun., 2472–2473.
Hojeij, M., Su, B., Tan, S.X., Mériguet, G., Girault, H.H., 2008. Acs Nano 2, 984–992.
Isarov, A.V., Chrysochoos, J., 1997. Langmuir 13, 3142–3149.
Kang, Q., Yang, L.X., Chen, Y.F., Luo, S.L., Wen, L.F., Cai, Q.Y., Yao, S.Z., 2010. Anal. Chem. 82, 9749–9754.
Klimov, V.I., 2003. Los Alamos Science 28, 214–220.
Lan, Y.W., Zhou, L.Y., Tong, Z.F., Pang, Q., Wang, F., Gong, F.Z., 2011. Mater. Sci 34, 1173–1177.
Li, R.X., Liu, Y.X., Li, X.J., Zhang, S., Wu, D., Zhang, Y., Wei, Q., Du, B., 2014. Biosens. Bioelectron 62, 315–319.
Li, Y.J., Ma, M.J., Zhu, J.J., 2012. Anal. Chem. 84, 10492–10499.
Liang, M.M., Guo, L.H., 2007. Environ. Sci. Technol. 41, 658–664.
Liang, M.M., Jia, S.P., Zhu, S.C., Guo, L.H., 2007. Environ. Sci. Technol. 42, 635–639.
Liang, M., Liu, S., Wei, M., Guo, L.H., 2006. Anal. Chem. 78, 621–623.
Liu, S.L., Li, C., Cheng, J., Zhou, Y.X., 2006. Anal. Chem. 78, 4722–4726.
Liu, X., Dai, Q., Austin, L., Coutts, J., Knowles, G., Zou, J.H., Chen, H., Huo, Q., 2008. J. Am. Chem. Soc. 130, 2780–2782.
Lu, W., Jin, Y., Wang, G., Chen, D., Li, J.H., 2008. Biosens. Bioelectron 23, 1534–1539.
Murphy, C.J., Coffer, J.L., 2002. Appl. Spectrosc. 56, 16A–27A.
Nasr, C., Kamat, P.V., Hotchandani, S., 1998. J. Phys. Chem. B 102, 10047–10056.
Nirmal, M., Brus, L., 1999. Accounts Chem. Res 32, 407–414.
Niu, C.G., Liu, J., Qin, P.Z., Zeng, G.M., Ruan, M., He, H., 2011. Anal. Biochem. 409, 244–248.
Pardo-Yissar, V., Katz, E., Wasserman, J., Willner, I., 2003. J. Am. Chem. Soc. 125, 622–623.
Qin, G.X., Zhao, S.L., Huang, Y., Jiang, J., Ye, F.G., 2012. Anal. Chem. 84, 2708–2712.
Qu, W.S., Liu, Y.Y., Liu, D.B., Wang, Z., Jiang, X.Y., 2011. Angew. Chem. 50, 3442–3445.
Sant, P.A., Kamat, P.V., 2002. Phys. Chem. Chem. Phys. 4, 198–203.
Shen, Q.M., Zhao, X.M., Zhou, S.W., Hou, W.H., Zhu, J.J., 2011. J. Phys. Chem. C 115, 17958–17964.
Su, B., Fermín, D.J., Abid, J.-P., Eugster, N., Girault, H.H., 2005. J. Electroanal. Chem. 583, 241–247.
Tang, D.P., Niessner, R., Knopp, D., 2009. Biosens. Bioelectron 24, 2125–2130.
Tang, L., Zeng, G.M., Shen, G.L., Li, Y.P., Zhang, Y., Huang, D.L., 2008. Environ. Sci. Technol. 42, 1207–1212.
Tokudome, H., Yamada, Y., Sonezaki, S., Ishikawa, H., Bekki, M., Kanehira, K., Miyauchi, M., 2005. Appl. Phys. Lett. 87, 213901–213903.
Tu, W.W., Lei, J.P., Wang, P., Ju, H.X., 2011. Chem.-Eur. J 17, 9440–9447.
Vogel, R., Hoyer, P., Weller, H., 1994. J. Phys. Chem. 98, 3183–3188.
Wang, G.L., Xu, J.J., Chen, H.Y., 2010. Nanoscale 2, 1112–1114.
Wang, G.L., Xu, J.J., Chen, H.Y., Fu, S.Z., 2009a. Biosens. Bioelectron 25, 791–796.
Wang, G.L., Yu, P.P., Xu, J.J., Chen, H.Y., 2009b. J. Phys. Chem. C 113, 11142–11148.
Yang, C.P., Chen, R.S., Chen, K.H., Chen, Y.P., 2002. J. Chin. Chem. Soc. 49, 927–934.
Yildiz, H.B., Freeman, R., Gill, R., Willner, I., 2008. Anal. Chem. 80, 2811–2816.
Zarei, H., Ghourchian, H., Eskandari, K., Zeinali, M., 2012. Anal. Biochem. 421, 446–453.
Zhao, W.W., Ma, Z.Y., Yu, P.P., Dong, X.Y., Xu, J.J., Chen, H.Y., 2011. Anal. Chem. 84, 917–923.